Chinese Chemical Letters 33 (2022) 4253–4256

Contents lists available at ScienceDirect

Chinese Chemical Letters

journal homepage: www.elsevier.com/locate/cclet

Circularly polarized luminescence of talarolactones (+)/(−)-A and (+)/(−)-C: The application of CPL-calculation in stereochemical assignment

Guiyang Xia[a], Lingyan Wang[a], Huan Xia[a], Yuzhuo Wu[a], Yanan Wang[b], Haiyu Hu[b,*], Sheng Lin[a,c,**]

[a] Key Laboratory of Chinese Internal Medicine of Ministry of Education and Beijing, Dongzhimen Hospital, Beijing University of Chinese Medicine, Beijing 100700, China
[b] State Key Laboratory of Bioactive Substance and Function of Natural Medicines, Institute of Materia Medica, Chinese Academy of Medical Sciences and Peking Union Medical College, Beijing 100050, China
[c] Key Laboratory for Qinghai-Tibet Plateau Phytochemistry of Qinghai Province, College of Pharmaceutical, Qinghai Nationalities University, Xining 810007, China

ARTICLE INFO

Article history:
Received 5 February 2022
Revised 8 March 2022
Accepted 8 March 2022
Available online 11 March 2022

Keywords:
Circularly polarized luminescence
Natural products
Stereochemical assignment
Talarolactones (+)/(−)-A
Talarolactones (+)/(−)-C

ABSTRACT

Two pairs of fluorescent natural products, talarolactones (+)/(−)-A and (+)/(−)-C [(+)/(−)-**1** and (+)/(−)-**2**], were discovered and characterized as a new family of circularly polarized luminescence-active small organic molecules (CPL-SOMs) with high fluorescence efficiency and fascinating CPL properties. The CPL ($|g_{lum}|$) levels of enantiomerically pure (+)/(−)-**1** and (+)/(−)-**2** in solution falls into the usual range (10^{-5}–10^{-3}) considering their pure organic nature, but the sign of CPL were found to be closely related to the absolute configuration of C-8. The high agreement of the measured CPL spectra of (+)/(−)-**1** and (+)/(−)-**2** with the time-dependent density functional theory (TDDFT) calculated ones demonstrated the usefulness of CPL-calculation as a unique method for stereochemical assignment. This study may open up a new perspective for the stereochemical studies and the future development of CPL materials.

Circularly polarized luminescence (CPL), which measures the differential of right- and left-circularly polarized spontaneous emission from intrinsically chiral fluorophore or fluorophore in a chiral environment, is extensively observed in nature [1–3] and it has been attracting increasing attentions in recent years [4–7]. Besides the CPL materials derived from synthesis, such as chiral lanthanide complexes [8,9], axial chirality biphenyl groups [10], [2.2]paracyclophane derivatives [11], helicenes [12–14], supramolecular and polymeric structures [15,16], natural products with a variety of structural features might also be the great resources of CPL small organic molecules (CPL-SOMs), which are considered to be a promising class of materials for applications of CPL. Nonetheless, natural CPL-SOMs has been poorly reported except for some simple cyclic ketones that used as model for theoretical researches [17,18].

Depending on the same general aspects of molecular structure, circular dichroism (CD) and CPL are mutually complementary probes for the structural features of chiral molecules. As the CPL is typically responsible to the excited state (S_1) to ground state (S_0) electronic transition, information obtained from CPL is more selective and specific than that from CD. However, due to the limitations of instruments and appropriate molecular models, studies on the CPL spectra-structure relationships have been heretofore rather limited [19–21] in contrast to the tremendous efforts that have been devoted to the CD. To date, there is few empirical rules for the explanation and/or prediction of CPL properties including the CPL signs [22,23], resulted in the limitation on theoretical investigation. Quantum chemical calculations of CPL have been used to interpret of CPL data of some basic chiral compounds and CPL emitters [24–26], indicating that it is possible to apply CPL-calculation in the stereochemical assignment. However, to the best of our knowledge, the application of CPL-calculation in the determination of absolute configuration of chiral carbons has poorly been addressed [27]. Therefore, with further investigation into the interpretation of CPL of chiral compounds, applications of CPL to

* Corresponding author.
** Corresponding author at: Key Laboratory of Chinese Internal Medicine of Ministry of Education and Beijing, Dongzhimen Hospital, Beijing University of Chinese Medicine, Beijing 100700, China.
E-mail addresses: haiyu.hu@imm.ac.cn (H. Hu), lsznn@bucm.edu.cn (S. Lin).

https://doi.org/10.1016/j.cclet.2022.03.032
1001-8417/

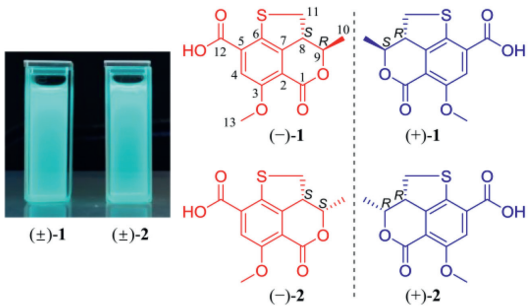

Fig. 1. Fluorescent images of (±)-**1** and (±)-**2** under UV light (365 nm) and chemical structures of (+)/(−)-**1** and (+)/(−)-**2**.

the structure elucidation may open up a new perspective for stereochemical studies.

Fungi are hyperdiverse and one of the best sources for natural pigments [17], however, natural skeletons with CPL properties have been rarely explored. As part of our ongoing effort to mining functional secondary metabolites from fungi [28–31], chemical investigations on a strain of endophytic fungus *Ophiosimulans tanaceti* were carried out. During the isolation process, a strong blue luminescence emission of a fraction under ultraviolet light radiation caught our attention, which prompted us to investigate the origins of the fluorescence. Eventually, two pairs of sulfur-containing isocoumarin derivates, talarolactones (+)/(−)-A and (+)/(−)-C [(+)/(−)-**1** and (+)/(−)-**2**] (Fig. 1), were characterized as a new family of CPL-SOMs with normal CPL levels ($|g_{lum}|$: $4.0 \times 10^{-4} \sim 5.1 \times 10^{-4}$) and strong fluorescent property (Φ_F: 42.17%–44.62%). The presence of chiral carbons in the structure is the only chiral element that responsible for their chiroptical dissymmetry, making them ideal molecular models for the study of CPL spectra-structure relationships. The systematic analysis of the signs of the CPL spectra, assisted by the time-dependent density functional theory (TDDFT) calculations, leading us to conclude that the right- and left- handed twist of the chromophores (consisting of the lactone C=O and aromatic ring) in the excited state exhibit (+)- and (−)-CPL, respectively. Further structure conformation analysis indicated that the absolute configuration of C-8 closely related to the dihedral angles (θ) between the chromophores.

Bearing all these ideas in mind, herein we present, for the first time, the application of CPL-calculations in stereochemical assignments. It was successfully applied to the determination of the stereoconfiguration of (−)-**1**, (+)-**1**, (−)-**2**, (+)-**2**, and some reported CPL-active SOMs [(1*S*,4*R*)-**3**, (1*R*,4*S*)-**3**, (−)-**4**, (+)-**4**, (−)-**5** and (+)-**5**]. We strongly believe that the results achieved with this work may represent an important milestone for the stereochemical studies and the future development of CPL materials.

Compound **1** was obtained as a yellow, amorphous powder, and possessed a molecular formula of $C_{13}H_{12}O_5S$ assigned by HRESIMS data for the $[M+H]^+$ ion at *m/z* 281.0477 (calcd. for $C_{13}H_{13}O_5S$, 281.0478), requiring 8 degrees of unsaturation. A detailed comparation of its UV, IR, and 1D- and 2D-NMR spectra with talarolactone A, which had been recently reported as an optically pure compound isolated from the endolichenic fungus *Talaromyces* sp., revealed that the planar structure of **1** should be identical with talarolactone a (Table S1 in Supporting information) [32]. However, negligible optical activity indicated that **1** was a pair of racemic mixture. Subsequent chiral resolution of **1** afforded the enantiomers (−)-**1** and (+)-**1**, displaying mirror image CD curves and opposite specific rotation [(−)-**1**: $[\alpha]_D^{25}$ −197.5 (*c* 0.12, MeOH); (+)-**1**: $[\alpha]_D^{25}$ +203.5 (*c* 0.09, MeOH)], and the final assignment of the absolute configurations of (−)-**1** (8*S*,9*R*) and (+)-**1** (8*R*,9*S*) were achieved by comparison of their experimental

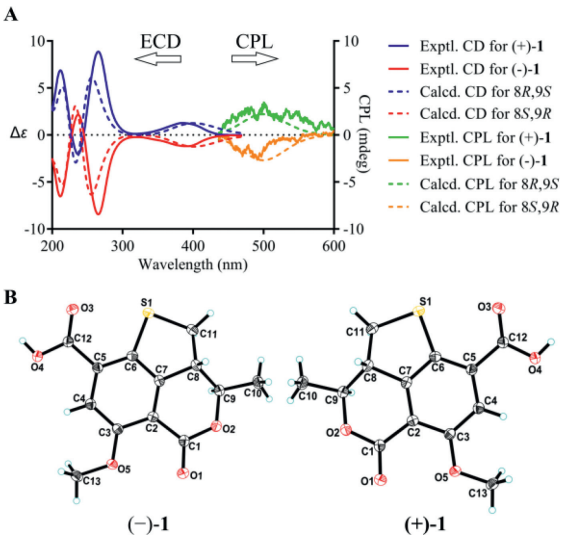

Fig. 2. (A) Experimental and computational ECD and CPL spectra for (−)-**1** and (+)-**1**. (B) X-ray ORTEP drawing of (−)-**1** and (+)-**1** depicting their absolute configurations.

CD spectra with TDDFT calculated ones combined with the analysis of their single-crystal X-ray diffraction data using Cu Kα radiation (Figs. 2A and B). Accordingly, the significant difference of the specific rotation between the (+)-**1** [$[\alpha]_D^{25}$ +203.5 (*c* 0.09, MeOH)] and talarolactone A [$[\alpha]_D^{25}$ +36.85 (*c* 0.445, MeOH)] concluded that the reported talarolactone A should be a partial racemic mixture, which was confirmed by its weak CD Cotton bands (especially for the first Cotton band around 385 nm, Fig. S13 in Supporting information). Consequently, the enantiomers (−)-**1** and (+)-**1** should be given the names of (−)-talarolactone A and (+)-talarolactone A, respectively.

Compound **2**, obtained as yellow powder, possesses the same molecular formula ($C_{13}H_{12}O_5S$) as **1**, as determined from NMR data and HRESIMS $[M+H]^+$ ion at *m/z* 281.0477 (calcd. for $C_{13}H_{13}O_5S$, 281.0478). The UV, IR, and CD data of **2** were also resembled to those of **1**. A side-by-side comparison of the ^1H and ^{13}C NMR data of **2** with those of **1** revealed that the only difference between **1** and **2** was the small change in chemical shifts from C-8 to C-11. These findings, combined with the 2D NMR data and the small coupling constant between H-8 and H-9 ($J = 6.4$ Hz), affirmed that **2** was the C-8−C-9 diastereomer of **1**. Since the small specific rotation of **2** [$[\alpha]_D^{25}$ +30.5 (*c* 0.08, MeOH)] was measured, its partial racemic nature was presumed and verified by the chiral HPLC separation. Subsequent preparation led to the acquisition of (−)-**2** [$[\alpha]_D^{25}$ −182.9 (*c* 0.04, MeOH)] and (+)-**2** [$[\alpha]_D^{25}$ +183.2 (*c* 0.13, MeOH)]. Finally, the absolute configurations of (−)-**2** and (+)-**2** were assigned as 8*S*,9*S* and 8*R*,9*R*, respectively, according to the comparing of the experimental and TDDFT-simulated CD spectra, as well as the single-crystal X-ray diffraction data of (+)-**2** (Figs. 3A and B).

With the observation of strong blue fluorescence under ultraviolet light radiation, (+)/(−)-**1** and (+)/(−)-**2** are responsible for the fluorescence fraction mentioned above. Then the photophysical properties of (+)/(−)-**1** and (+)/(−)-**2** were studied. Each of (+)/(−)-**1** and (+)/(−)-**2** showed the longest wavelength UV absorbance at approximately 395 nm and fluorescence emission centered at approximately 480 nm (Figs. S14 and S28 in Supporting information) with high fluorescence quantum yields (ϕ_F) in MeOH ranged between 42.17% and 44.62%, and the fluorescence lifetime (τ_s) of (−)-**1**, (+)-**1**, (−)-**2** and (+)-**2** were determined to be 8.81, 9.13, 14.12, and 14.15 ns, respectively. Interestingly, when the living HO-8910 cells were treated with (±)-**1** and (±)-**2** at 50 μmol/L for

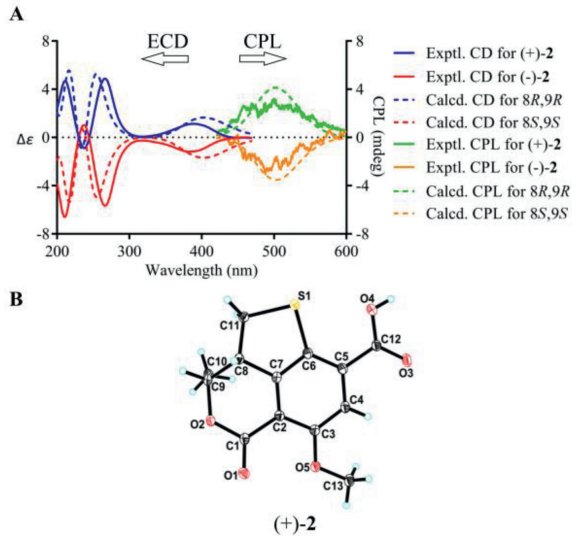

Fig. 3. (A) Experimental and computational ECD and CPL spectra for (−)-**2** and (+)-**2**. (B) X-ray ORTEP drawing of (+)-**2** depicting its absolute configuration.

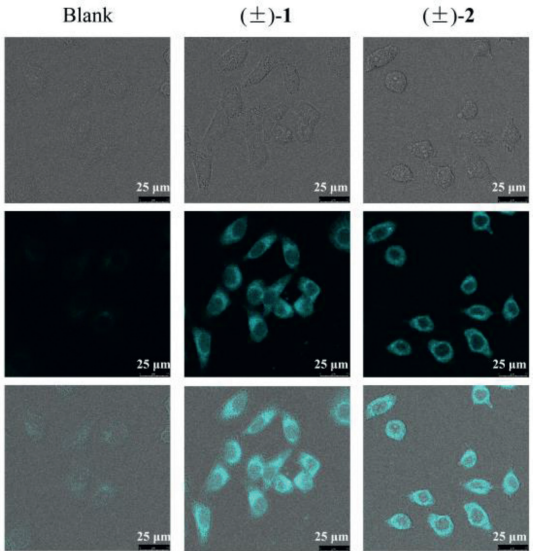

Fig. 4. Representative cellular fluorescence imaging of HO-8910 cells treated with (±)-**1** and (±)-**2**. (1) brightfield (top); (2) blue channel λ_{ex} = 405 nm (middle); (3) merged (bottom).

0.5 h, (±)-**1** and (±)-**2** could readily accumulated in the cells without cytotoxicity as shown in the cellular images (Fig. 4), heralding their promising application in cellular imaging.

Considering the presence of chiral elements in the structures of the enantiomers, we also investigated the CPL properties of (+)/(−)-**1** and (+)/(−)-**2** to further explore their potential applications. To our delight, virtually mirror images of CPL spectra and almost opposite g_{lum} values were detected for each pair of enantiomers, and the emission wavelengths of the CPL signals correspond well to the fluorescence emission wavelengths. In addition, the signs of the CPL were identical to their first Cotton CD band (lowest-energy band), which is in consistent with the general trends for the CD and CPL spectra (Figs. 2A and 3A). To the best of our knowledge, they were the first examples of natural fluorescent SOMs that demonstrate CPL activity controlled by chiral carbon with a high fluorescence quantum yield.

To further shed light on the photophysical and chiroptical properties of (+)/(−)-**1** and (+)/(−)-**2**, we conducted the DFT and

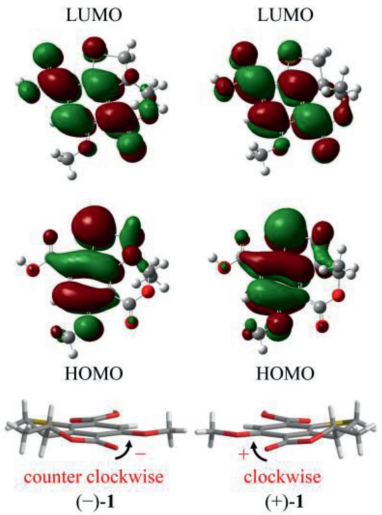

Fig. 5. Calculated HOMOs and LUMOs of (−)-**1** and (+)-**1**, and the relation between the twist arrangement of the key chromophores and the respective positive or negative CPL signatures.

TDDFT calculations at the B3LYP/6-311G+(d,p) level. Based on the calculated geometries in the S_0 and S_1 states, the entire structural difference was mainly attributed to the change of the dihedral angle between the lactone C=O and the benzene ring (Table S9 in Supporting information). The highest occupied molecular orbitals (HOMOs) and the lowest unoccupied molecular orbitals (LUMOs) of (+)/(−)-**1** and (+)/(−)-**2** (Fig. 5 and Fig. S38 in Supporting information) were all delocalized over the entire skeleton, with a slightly less distribution on the lactone carbonyl in the HOMOs. Besides, the CPL and the first Cotton CD band related transitions between S_0 and S_1 were attributed to the electronic transition between HOMOs and LUMOs. Thus, the chiroptical response were probably related to the planar asymmetry of the lactone ring.

Detailed analysis of the structural constructions revealed that the signs of the CPL could be interpreted from the direction of the twist of the lactone C=O and the benzene ring, namely, clockwise- and counter clockwise-twist exhibit (+)- and (−)-CPL, respectively (Fig. 5). Similar twist rule has been apparent in the explanation of some Cotton effects in CD spectra, but now turned out to be also applicable to the CPL signs. Recently, several related approaches for other chromophores have been reported. Considering the relatively rigid structures of (+)/(−)-**1** and (+)/(−)-**2**, it could be easily speculated that the signs of their CPL were also restricted to the absolute configuration of C-8, and it was confirmed by the well matched calculated and experimental CPL spectra (Figs. 2A and 3A).

Motived by our successful CPL-calculation for **1** and **2**, it could be speculated that the application of the CPL-calculation might be a promising unique method for the stereochemical assignment as a supplementary of CD-calculation. To verify this speculation and the reliability of our calculation method, TDDFT calculations of the fluorescence and CPL properties of the literature reported CPL-SOMs, (1*S*,4*R*)-camphorquinone [(1*S*,4*R*)-**3**] and (1*R*,4*S*)-camphorquinone [(1*R*,4*S*)-**3**] (Fig. 6) [25], were performed. As expected, both the calculated fluorescence (Fig. S39 in Supporting information) and CPL spectra (Fig. S40 in Supporting information) met well with their reported experimental and theoretical calculation results, which verified our CPL-calculation method and made the absolute configuration of (1*S*,4*R*)-**3** and (1*R*,4*S*)-**3** successfully distinguished.

To further extend the application scope of the CPL-calculation, another pair of CPL-SOMs, (+)-10,10′-spirobi(indeno[1,2-*b*][1]benzothiophene) [(+)-**4**] and (−)-10,10′-spirobi(indeno[1,2-

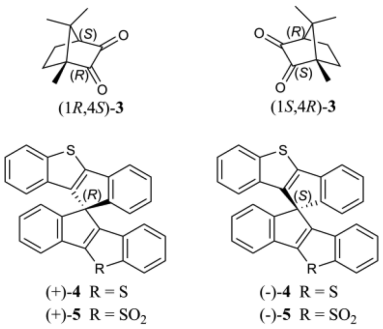

Fig. 6. Chemical structures of compounds **3**–**5**.

b][1]benzothiophene) [(−)-**4**] [33], were introduced to our investigation. (+)-**4** and (−)-**4** were reported as a pair of spiro-chiral enantiomers which showed mirror image CPL curves; however, their absolute configurations were not determined by the authors. To assign the absolute configuration, we calculated the CPL spectra of (+)-**4** and (−)-**4**, which fully agreed with their experimental CPL information. By this approach, the absolute configurations of (+)-**4** and (−)-**4** could be assigned as *R* and *S*, respectively, which was confirmed by the ECD-calculations (Figs. S41 and S42 in Supporting information). Simultaneously, the absolute configurations of another pair of CPL-SOMs, (+)-10,10′-spirobi(indeno[1,2-*b*][1]benzothiophene) 5,5-dioxide and (−)-10,10′-spirobi(indeno[1,2-*b*][1]benzothiophene) 5,5-dioxide [(+)-**5** and (−)-**5**] [33], were determined by CPL-calculation (Figs. S43 and S44 in Supporting information). Consequently, the above findings demonstrated that the CPL-calculation method is straightforward and reliable, and it can be applied for the determination of absolute configuration of chiral carbons.

It has been over seventy years since the first measurement of CPL activity, however, to the best of our knowledge, this work presents the first proofs of natural fluorescent SOMs that demonstrate CPL properties. In contrast to the reported CPL emitters that generate CPL from the dissymmetry of different aromatic planes, (+)/(−)-**1** and (+)/(−)-**2** represent a new family of CPL-SOMs. We strongly believe that, although with moderate $|g_{lum}|$ values, here reported can be considered as a starting point for the discovery of CPL-SOMs from natural products.

Remarkably, the results of TDDFT calculations shed further light on the CPL spectra-structure relationships and an important step forward of the application of CPL-calculation to the stereochemical studies has been taken. As CPL reflects the structural properties of the luminescent excited states, the more selective and specific CPL-calculations might be a powerful supplement of the NMR/OR/ECD/VCD-calculations in the stereochemical studies and the stereochemical studies is herein extended to the excited states. In addition, with only the excited states responsible for the CPL being calculated, CPL-calculations will be more efficient than the NMR/OR/ECD/VCD-calculations, and the computational expense will be much reduced.

Declaration of competing interest

The authors declare no conflict of interest.

Acknowledgments

This work was supported by the National Natural Science Foundation of China (Nos. 81803397, 82073978 and 22122705), Beijing Natural Science Foundation (No. JQ18026) and Innovation Team of Medicinal Material Resource Protection and High Value Utilization in Qinghai Province (No. 2021XJPI02).

Supplementary materials

Supplementary material associated with this article can be found, in the online version, at doi:10.1016/j.cclet.2022.03.032.

References

[1] I.M. Daly, M.J. How, J.C. Partridge, et al., Nat. Commun. 7 (2016) 12140.
[2] J. Bailey, Science 281 (1998) 672–674.
[3] H. Wynberg, E.W. Meijer, J.C. Hummelen, et al., Nature 286 (1980) 641–642.
[4] J.L. Ma, Q. Peng, C.H. Zhao, Chem. Eur. J. 25 (2019) 15441–15454.
[5] M. Li, M.Y. Wang, Y.F. Wang, et al., Angew. Chem. Int. Ed. 60 (2021) 20728–20733.
[6] C. Wang, T. Jiang, X. Ma, Chin. Chem. Lett. 31 (2020) 2921–2924.
[7] S. Jiang, S. Zhou, Y. Chen, et al., Chin. Chem. Lett. 33 (2022) 2442–2446.
[8] J. Zhang, L. Dai, A.M. Webster, et al., Angew. Chem. Int. Ed. 60 (2021) 1004–1010.
[9] R. Carr, N.H. Evans, D. Parker, Chem. Soc. Rev. 41 (2012) 7673–7686.
[10] J. Han, D. Yang, X. Jin, et al., Angew. Chem. Int. Ed. 58 (2019) 7013–7019.
[11] C.H. Chen, W.H. Zheng, Org. Lett. 23 (2021) 5554–5558.
[12] H.W. Li, M. Li, Z.H. Zhao, et al., Org. Lett. 23 (2021) 4759–4763.
[13] F. Zhou, Z. Huang, Z. Huang, et al., Org. Lett. 23 (2021) 4559–4563.
[14] W.-B. Lin, M. Li, L. Fang, et al., Chin. Chem. Lett. 29 (2018) 40–46.
[15] O. Oki, C. Kulkarni, H. Yamagishi, et al., J. Am. Chem. Soc. 143 (2021) 8772–8779.
[16] L. Wang, L. Yin, W. Zhang, et al., J. Am. Chem. Soc. 139 (2017) 13218–13226.
[17] R. Duval, C. Duplais, Nat. Prod. Rep. 34 (2017) 161–193.
[18] H Tanaka, Y Inoue, T Mori, ChemPhotoChem 2 (2018) 386–402.
[19] C.A. Emeis, L.J. Oosterhoff, Chem. Phys. Lett. 1 (1967) 129–132.
[20] H.P.J.M. Dekkers, L.E. Closs, J. Am. Chem. Soc. 98 (2002) 2210–2219.
[21] C.K. Luk, F.S. Richardson, J. Am. Chem. Soc. 96 (2002) 2006–2009.
[22] K. Dhbaibi, L. Favereau, M. Srebro-Hooper, et al., Chem. Sci. 9 (2018) 735–742.
[23] K. Takaishi, K. Iwachido, R. Takehana, et al., J. Am. Chem. Soc. 141 (2019) 6185–6190.
[24] H. Tanaka, M. Ikenosako, Y. Kato, et al., Commun. Chem. 1 (2018) 38.
[25] G. Longhi, E. Castiglioni, S. Abbate, et al., Chirality 25 (2013) 589–599.
[26] B. Pritchard, J. Autschbach, ChemPhysChem 11 (2010) 2409–2415.
[27] A. Mandi, T. Kurtan, Nat. Prod. Rep. 36 (2019) 889–918.
[28] Y.Z. Wu, G.Y. Xia, H. Xia, et al., J. Nat. Prod. 85 (2022) 248–255.
[29] G.Y. Xia, L.Y. Wang, J.F. Zhang, et al., Chin. J. Nat. Med. 18 (2020) 75–80.
[30] Y.Z. Wu, H.W. Zhang, Z.H. Sun, et al., Eur. J. Med. Chem. 145 (2018) 717–725.
[31] Y.N. Wang, G.Y. Xia, L.Y. Wang, et al., Org. Lett. 20 (2018) 7341–7344.
[32] W.H. Yuan, M.T. Teng, Y.F. Yun, et al., J. Nat. Prod. 83 (2020) 1716–1720.
[33] K. Takase, K. Noguchi, K. Nakano, Org. Lett. 19 (2017) 5082–5085.